



Original Article

Theoretical study of cross sections of proton-induced reactions on cobalt

Mustafa Yiğit

Department of Physics, Aksaray University, 68100, Aksaray, Turkey

ARTICLE INFO

Article history:

Received 14 May 2017

Received in revised form

28 October 2017

Accepted 9 January 2018

Available online 1 February 2018

Keywords:

Cobalt

Nuclear Structural Materials

Reaction Cross Section

TENDL Database

ABSTRACT

Nuclear fusion may be among the strongest sustainable ways to replace fossil fuels because it does not contribute to acid rain or global warming. In this context, activated cobalt materials in corrosion products for fusion energy are significant in determination of dose levels during maintenance after a coolant leak in a nuclear fusion reactor. Therefore, cross-section studies on cobalt material are very important for fusion reactor design. In this article, the excitation functions of some nuclear reaction channels induced by proton particles on ^{59}Co structural material were predicted using different models. The nuclear level densities were calculated using different choices of available level density models in ALICE/ASH code. Finally, the newly calculated cross sections for the investigated nuclear reactions are compared with the experimental values and TENDL data based on TALYS nuclear code.

© 2018 Korean Nuclear Society, Published by Elsevier Korea LLC. This is an open access article under the CC BY-NC-ND license (<http://creativecommons.org/licenses/by-nc-nd/4.0/>).

1. Introduction

Nuclear fusion energy as the world's primary energy source may be among the strongest sustainable ways to replace fossil fuels. Nuclear fusion is able to supply considerable amounts of energy over millions of years. Therefore, it is potentially a very attractive source of energy [1]. Clearly, the high temperature and intensive radiation in a nuclear fusion reactor can cause damage to the structural materials. Therefore, the design and structural material selection of fusion reactors are very important. In this framework, the cross sections of nuclear reactions induced by nucleons are required for the design calculations in fusion reactors and other related investigations. Because of their high strength and hardness properties, cobalt-based alloys have been used as structural materials in nuclear reactors [2–4]. In fact, activated cobalt materials in corrosion products are significant in determination of dose levels during maintenance after a coolant leak at a nuclear fusion reactor. Cobalt materials for water cooling devices are the principal parts of activated corrosion products [3]. On the other hand, cross-section data are needed for many applications, such as fusion, fission, accelerator-driven applications, dosimetry, and nuclear medical applications [5]. Particularly, the reaction processes occurring in nuclear fusion reactors should be well known. In this context, many models have been developed for better understanding of these

processes. Various nuclear models have been used to investigate the different reaction mechanisms associated with reactor design and material selection. These models also provide several advantages in terms of cost and time [6–9]. Because the initial testing phase of the International Fusion Material Irradiation Facility may use H^+ or H_2^+ , the nuclear reactions induced by protons need to be considered. Therefore, the International Fusion Material Irradiation Facility needs high accuracy evaluated proton data for prediction of potential radiation hazards from beam transport elements and accelerating cavities [10,11]. An accurate model description of each nuclear reaction channel is important for understanding the formation and decay of compound nuclei. It is known that the compound process for a nuclear reaction defines the low-energy portion of the function [12,13]. On the other hand, with increasing incident energy, the precompound process becomes more important [14–16].

Nuclear excitation functions of the $^{59}\text{Co}(p,n)^{59}\text{Ni}$, $^{59}\text{Co}(p,n3p)^{56}\text{Mn}$, $^{59}\text{Co}(p,2np)^{57}\text{Co}$, $^{59}\text{Co}(p,3n)^{57}\text{Ni}$, $^{59}\text{Co}(p,3np)^{56}\text{Co}$, $^{59}\text{Co}(p,4n)^{56}\text{Ni}$, and $^{59}\text{Co}(p,4np)^{55}\text{Co}$ reactions in this article were calculated using the code ALICE/ASH [12]. In addition, a complete analysis of cross sections calculated from different level density models such as the Fermi Gas model (FGM) with an energy-dependent level density parameter [17], the FGM with an energy-independent level density parameter, the superfluid nuclear model (SFM) [18], and the Kataria–Ramamurthy FGM (KRM) [19] were presented. Furthermore, the new excitation functions of nuclear reactions induced by proton particles on

E-mail address: mustafayigit@aksaray.edu.tr.

^{59}Co structural material were estimated with different input parameters and were also compared with the measured cross-section data reported in the literature [20] and in the TENDL database [21].

2. Materials and methods

It should be stated that different nuclear reaction channels occur with different probabilities. Physically, the reaction probability is expressed in terms of a quantity called nuclear cross section. The shapes of nuclear cross sections can be predicted using reaction models in nuclear codes. Consequently, these models are needed to obtain educated guesses of the excitation functions. Nuclear reaction codes for the decay of compound nucleus are a useful way to predict and interpret yields for different reactions. These codes, combining compound and precompound decay channels, are very successful for cross-section calculations at a wide range of incident energies. In addition, one of the important inputs to the reaction cross-section calculations is the nuclear level density. Until this time, studies on nuclear reactions indicate that the nuclear level density models are necessary to explain the excitation function of reactions. The level density is the number of nuclear excited levels around the excitation energy. The nuclear excited levels at low excitation energies are discrete; however, they appear to represent a continuum with increasing excitation energy. Consequently, a model for calculating the nuclear level densities is needed in the continuum energy regime. In the same context, at both low and high excitation energy regions, a correct and reliable description of the excited levels of a nucleus has been used to test the success of the nuclear reaction model including cross-section calculations [22].

Level densities for equilibrium states can be calculated using different approaches in the ALICE/ASH code. The most widely used level density expression in nuclear codes is the FGM of Bethe. The inadequacy of this model for nuclei close to shell closures is known [19]. The KRM has brought out the significant contribution of the surface-to-volume ratio of a nucleus to its nuclear level density parameter, deduced from the measured values. This model is expressed in terms of a Fourier expansion of the single particle level density of nucleons in the nucleus. The single particle level density as the macroscopic part of the nuclear level density parameter is related to the average density of the single particle states at the Fermi energy. The nuclear level density parameter in this model was written as follows:

$$a = \alpha A \left(1 - \beta A^{-\frac{1}{3}} \right) \quad (1)$$

The parameter “ a ” is dependent on the well parameters and also can be parameterized by the nucleus separation energies, as follows:

$$a = \alpha A + A^{\frac{2}{3}} \left[\beta_0 + \frac{\beta_1}{S_n} + \frac{\beta_2}{S_p} \right] \quad (2)$$

The terms α , β_0 , β_1 , and β_2 are the fitting parameters. The terms S_p and S_n are the proton and neutron separation energies, respectively [19].

The nuclear level densities in the FGM with energy-independent level density parameters are calculated as follows:

$$\rho(U) \propto (U - \delta)^{-5/4} e^{(2\sqrt{a(U-\delta)})} \quad (3)$$

The nuclear level density parameter “ a ” is equal to A/y . Here, “ y ” and “ A ” are a constant and the mass number of the nucleus, respectively. “ δ ” and “ U ” represent pairing correction and excitation energy, respectively [12].

The nuclear level densities in the FGM with the energy-dependent level density parameter proposed by Ignatyuk et al. [17] are calculated as follows:

$$\rho(U) \propto a^{-1/4} (U - \delta)^{-5/4} e^{(2\sqrt{a(U-\delta)})} \quad (4)$$

The nuclear level density parameter $a(U)$, generally referred to as the Ignatyuk formula, is written as follows [17]:

$$a(U) = \tilde{a} \left(1 + \frac{f(U)\delta W}{U} \right) \quad (5)$$

where the quantity “ δW ” denotes the shell correction. The function “ $f(U)$ ” is equal to $1 - e^{-\gamma U}$. The quantity “ \tilde{a} ” is the asymptotic value of the nuclear level density parameter and is equal to $A(\alpha + \beta A)$.

where the coefficients $\gamma = 0.054 \text{ MeV}^{-1}$; $\beta = -6.3 \cdot 10^{-5}$; $\alpha = 0.154$.

The pairing correction is equal to $\delta = 0$ for odd–odd nuclei and $12/A^{1/2}$ for nuclei with odd A ; $\delta = 24/A^{1/2}$ for even–even nuclei [12,17].

The nuclear level densities according to the SFM are calculated as follows [18]:

$$\rho(U) = \rho_{qp}(U') K_{vib}(U') K_{rot}(U') \quad (6)$$

where $\rho_{qp}(U')$ represents the density of quasi particle nuclear excitation. Here, $K_{rot}(U')$ and $K_{vib}(U')$ are rotational and vibrational enhancement factors at effective energy of U' excitation, respectively [18]. Level density parameters in the SFM are written as follows:

$$a(U) = \begin{cases} \tilde{a}(1 + \delta W \varphi(U' - E_{cond}) / (U' - E_{cond})), & U' > U_{cr} \\ a(U_{cr}), & U' \leq U_{cr} \end{cases} \quad (7)$$

The critical energy of the phase transition, $U_{cr} = 0.472a(U_{cr})\Delta_0^2 - n\Delta_0$; the effective energy, $U' = U - n\Delta_0$; the condensation energy, $E_{cond} = 0.152a(U_{cr})\Delta_0^2 - n\Delta_0$. The correlation function “ Δ_0 ” is equal to $12A^{-1/2}$ [12,18].

3. Results

In this work, the nuclear cross-section data of the $^{59}\text{Co}(p,n)^{59}\text{Ni}$, $^{59}\text{Co}(p,n3p)^{56}\text{Mn}$, $^{59}\text{Co}(p,2np)^{57}\text{Co}$, $^{59}\text{Co}(p,3n)^{57}\text{Ni}$, $^{59}\text{Co}(p,3np)^{56}\text{Co}$, $^{59}\text{Co}(p,4n)^{56}\text{Ni}$, and $^{59}\text{Co}(p,4np)^{55}\text{Co}$ reactions were calculated in the ALICE/ASH code using the KRM, FGM, and SFM level densities.

3.1. $^{59}\text{Co}(p,n)^{59}\text{Ni}$ nuclear reaction

Fig. 1 shows the excitation curves for the $^{59}\text{Co}(p,n)^{59}\text{Ni}$ reaction up to 30 MeV. The excitation functions for this nuclear reaction give maximum values in the energy range of 7–17 MeV. At low incident energies, the KRM and FGM [with $a(U)$] calculations have different cross-section data than those of the other excitation functions. The experimental data of Kailas et al. [23] and Johnson et al. [24] for the investigated reaction are quite a bit lower than the cross section calculations with SFM and FGM (with expression $a = A/K$) level densities. Moreover, the excitation function reported by Albert [25] at incident proton energies of 3.6–8.1 MeV yield an acceptable harmony with the SFM and FGM (with expression $a = A/K$) calculations and TENDL-2015 data. Besides this, the measured excitation function of Hansen and Albert [26] tends to be a bit lower than the cross-section calculation results with KRM level density using the ALICE/ASH code. The model-based calculations predicted using the KRM level density agree satisfactorily well with the experimental data reported by Chodil et al. [27] in the energy range of 7–15 MeV.

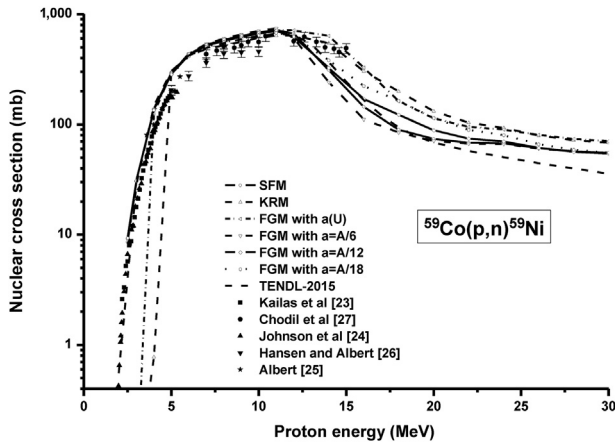


Fig. 1. The theoretically calculated and experimentally measured excitation curves for $^{59}\text{Co}(p,n)^{59}\text{Ni}$ reaction. FGM, Fermi Gas model; KRM, Kataria–Ramamurthy Fermi Gas model; SFM, superfluid nuclear model.

3.2. $^{59}\text{Co}(p,n3p)^{56}\text{Mn}$ nuclear reaction

Comparison of the model-based excitation curves with the experimental data of Sharp et al. [28] for $^{59}\text{Co}(p,n3p)^{56}\text{Mn}$ nuclear reaction is presented in Fig. 2 as a function of proton energies up to 100 MeV. The nuclear cross sections from model calculations appear to give maximum values at bombarding proton energy of about 60 MeV. As can be seen in Fig. 2, the FGM calculation results with level density parameter of $a = A/18$ for the considered reaction have good agreement with the four experimental data points reported by Sharp et al. [28] in the energy range of 83.6–99.1 MeV. The cross sections predicted from the different level density parameters (with expression $a = A/K$) in the ALICE/ASH computer code give different results, in general.

3.3. $^{59}\text{Co}(p,2np)^{57}\text{Co}$ nuclear reaction

The nuclear cross sections for the $^{59}\text{Co}(p,2np)^{57}\text{Co}$ nuclear reaction in the present article are shown in Fig. 3 for incident proton energies up to 100 MeV. The excitation functions have a broad peak with a maximum value of about 728 mb at proton energy of 36 MeV. As can be seen in Fig. 3, the experimental data obtained by Sharp et al. [28] have lower cross-section values than the ALICE/ASH code calculations and TENDL-2015 database data, particularly

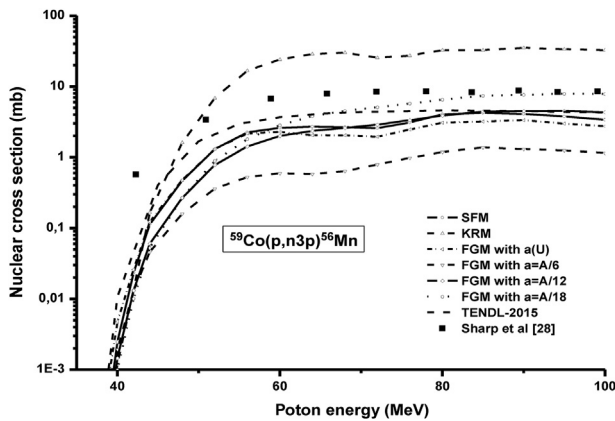


Fig. 2. The theoretically calculated and experimentally measured excitation curves for $^{59}\text{Co}(p,n3p)^{56}\text{Mn}$ reaction. FGM, Fermi Gas model; KRM, Kataria–Ramamurthy Fermi Gas model; SFM, superfluid nuclear model.

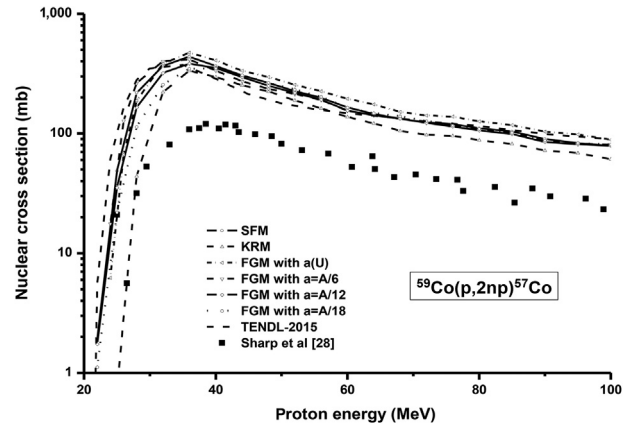


Fig. 3. The theoretically calculated and experimentally measured excitation curves for $^{59}\text{Co}(p,2np)^{57}\text{Co}$ reaction. FGM, Fermi Gas model; KRM, Kataria–Ramamurthy Fermi Gas model; SFM, superfluid nuclear model.

at incident energies above 30 MeV. However, the cross-section values measured by Sharp et al. [28] at the incident energies of 26.5 MeV, 28 MeV, and 29.5 MeV are in very good agreement with the cross-section results predicted using the KRM level density for this reaction.

3.4. $^{59}\text{Co}(p,3n)^{57}\text{Ni}$ nuclear reaction

The cross sections of the $^{59}\text{Co}(p,3n)^{57}\text{Ni}$ nuclear reaction are shown in Fig. 4 for the incident proton energies up to 100 MeV. It may be pointed out that the excitation functions calculated from different level density models in the ALICE/ASH code give different results. The excitation function predicted using the KRM level density in the ALICE/ASH code is found to have good agreement with the cross-section data measured by Sharp et al. [28] in the proton energy range of 27.5–50.4 MeV. It is said that the excitation functions predicted by SFM and FGM level densities are at higher energies than those of the KRM prediction and the data of Sharp et al. [28]. Particularly, the TENDL-2014 excitation function for this reaction has low cross-section values above the incident energy of ~ 40 MeV. Moreover, the KRM predictions by the ALICE/ASH code show excellent harmony with the experimental data of Ditroi et al. [29] in the energy range of 59.7–69.8 MeV. Besides this, the

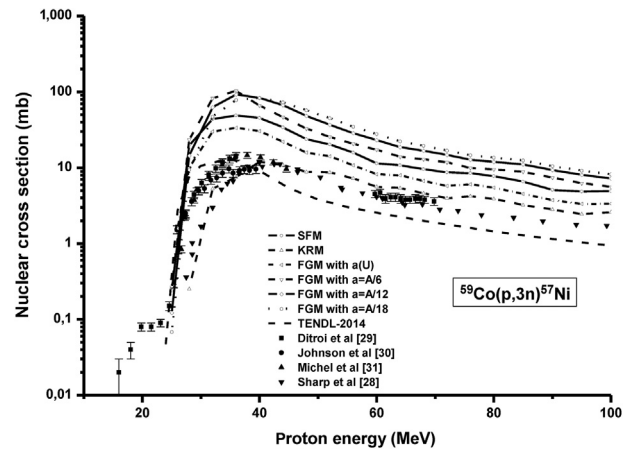


Fig. 4. The theoretically calculated and experimentally measured excitation curves for $^{59}\text{Co}(p,3n)^{57}\text{Ni}$ reaction. FGM, Fermi Gas model; KRM, Kataria–Ramamurthy Fermi Gas model; SFM, superfluid nuclear model.

cross-section predictions calculated by the KRM level density show good agreement with the data reported by Johnson et al. [30] and Michel et al. [31] at the incident energies above ~ 30 MeV.

3.5. $^{59}\text{Co}(p,3np)^{56}\text{Co}$ nuclear reaction

The model-based calculation data for the $^{59}\text{Co}(p,3np)^{56}\text{Co}$ reaction are presented in Fig. 5 together with the experimental results of Sharp et al. [28]. The nuclear excitation functions calculated by ALICE/ASH code appear to give maximum values at the incident proton energy of 40–50 MeV. In general, the TENDL-2015 data based on TALYS code and the cross-section predictions with the KRM level density in the ALICE/ASH computer code for $^{59}\text{Co}(p,3np)^{56}\text{Co}$ nuclear reaction seem to be in good agreement with the measured data of Sharp et al. [28], except for a few cross-section data points. It is observed that the effect of the variation of nuclear level densities on the calculated cross sections is quite dominant in the maximum region of the excitation function.

3.6. $^{59}\text{Co}(p,4n)^{56}\text{Ni}$ nuclear reaction

The calculated and measured cross-section data of the $^{59}\text{Co}(p,4n)^{56}\text{Ni}$ nuclear reaction are presented in Fig. 6. It has also been pointed out that the FGM predictions [with $a(U)$] using the

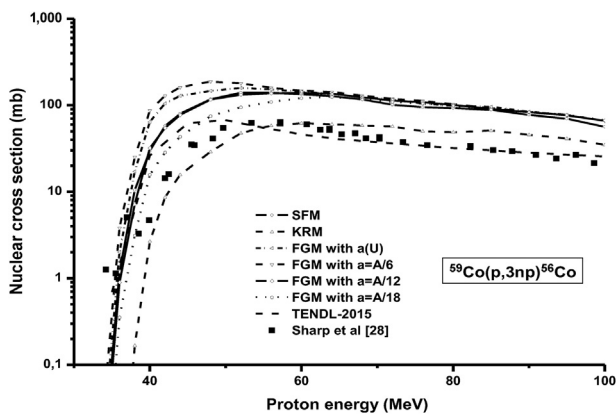


Fig. 5. The theoretically calculated and experimentally measured excitation curves for $^{59}\text{Co}(p,3np)^{56}\text{Co}$ reaction.

FGM, Fermi Gas model; KRM, Kataria–Ramamurthy Fermi Gas model; SFM, superfluid nuclear model.

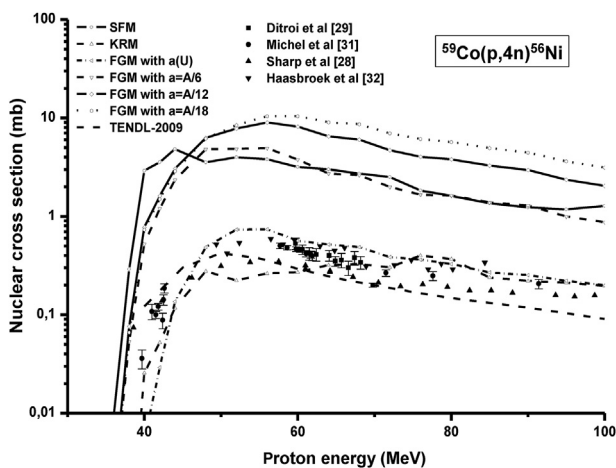


Fig. 6. The theoretically calculated and experimentally measured excitation curves for $^{59}\text{Co}(p,4n)^{56}\text{Ni}$ reaction.

FGM, Fermi Gas model; KRM, Kataria–Ramamurthy Fermi Gas model; SFM, superfluid nuclear model.

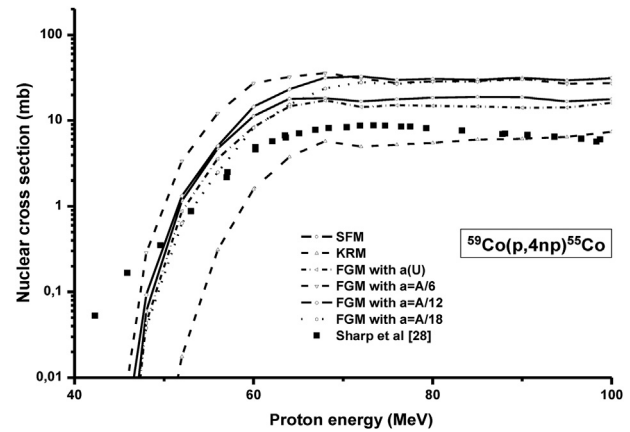


Fig. 7. The theoretically calculated and experimentally measured excitation curves for $^{59}\text{Co}(p,4np)^{55}\text{Co}$ reaction.

FGM, Fermi Gas model; KRM, Kataria–Ramamurthy Fermi Gas model; SFM, superfluid nuclear model.

ALICE/ASH code are in good agreement with the cross-section values reported by Haasbroek et al. [32] in the proton energy range of 49.4–84.4 MeV for the $^{59}\text{Co}(p,4n)^{56}\text{Ni}$ reaction. Generally, the KRM and FGM predictions [with $a(U)$] show good harmony with the cross sections measured by Ditroi et al. [29] and Michel et al. [31]. It can be seen in Fig. 6 that the TENDL-2009 excitation function based on the TALYS code shows good harmony with the experimental data of Sharp et al. [28]. As can be seen from Fig. 6, the excitation functions calculated with different level density parameters in the FGM have different cross-section results.

3.7. $^{59}\text{Co}(p,4np)^{55}\text{Co}$ nuclear reaction

Fig. 7 shows the theoretical and experimental calculations of the $^{59}\text{Co}(p,4np)^{55}\text{Co}$ nuclear reaction for incident proton energies up to 100 MeV. The calculated nuclear excitation curves for the considered nuclear reaction are almost constant above 60 MeV. It can be seen in Fig. 7 that the KRM estimations in the ALICE/ASH code for the $^{59}\text{Co}(p,4np)^{55}\text{Co}$ reaction yield an acceptable harmony with the measurements of Sharp et al. [28] above the proton energies of 65 MeV. The calculated nuclear excitation curves are almost constant above 60 MeV. It may be pointed out that the variation of nuclear level densities in the ALICE/ASH code has considerable influence on the predicted cross sections.

4. Discussion

The excitation curves of nuclear reactions induced by protons on the ^{59}Co nucleus have been calculated using the ALICE/ASH code. The impacts on the calculated excitation functions of different nuclear level densities were analyzed for the investigated reactions. KRM takes into account the shell effects in the level densities. The model-based calculations with the KRM level density agree satisfactorily well with the measured data for the $^{59}\text{Co}(p,n)^{59}\text{Ni}$, $^{59}\text{Co}(p,3n)^{57}\text{Ni}$, $^{59}\text{Co}(p,3np)^{56}\text{Co}$, $^{59}\text{Co}(p,4n)^{56}\text{Ni}$, and $^{59}\text{Co}(p,4np)^{55}\text{Co}$ nuclear reactions at the high-energy tail portion of the excitation function. Cobalt-59 is also very close to the shell closures. The results indicate that the shell effects are very important to explain the excitation functions of proton-induced nuclear reactions. The TENDL database as a nuclear data library provides the output of the TALYS nuclear reaction code in the evaluated nuclear data file (ENDF) format. Generally, TENDL data for the $^{59}\text{Co}(p,n)^{59}\text{Ni}$, $^{59}\text{Co}(p,3n)^{57}\text{Ni}$, $^{59}\text{Co}(p,3np)^{56}\text{Co}$, and $^{59}\text{Co}(p,4n)^{56}\text{Ni}$ reactions show good harmony with the

experimental data. The nuclear level density model is a good parameter for characterizing the emission process of a nuclear reaction. It is observed that the accurate choice of level density model and level density parameter leads to better estimation of the excitation functions of nuclear reactions.

5. Conflicts of interest

Author declares there is no conflicts of interest.

References

- [1] S.C. Cowley, The quest for fusion power, *Nat. Phys.* 12 (2016) 384.
- [2] M. Yiğit, A. Kara, *Nucl. Eng. Tech.* 49 (2017) 996–1005.
- [3] B. Demir, A. Kaplan, V. Çapalı, *J. Fusion Energy* 34 (2015) 636.
- [4] M. Yiğit, *Appl. Radiat. Isot.* 105 (2015) 15–19.
- [5] Z.D. Wu, H.Y. Liang, Y.L. Han, *Nucl. Sci. Tech.* 27 (2016) 102.
- [6] M. Yiğit, E. Tel, I.H. Sarpün, *Nucl. Instrum. Meth. Phys. Res. B* 385 (2016) 59–64.
- [7] M. Yiğit, E. Tel, *Ann. Nucl. Energy* 69 (2014) 44–50.
- [8] M. Yiğit, E. Tel, *Nucl. Eng. Design* 293 (2015) 97–104.
- [9] M. Yiğit, E. Tel, *J. Radioanal. Nucl. Chem.* 306 (2015) 203–211.
- [10] E. Simeckova, P. Bem, M. Honusek, et al., *Phys. Rev. C* 84 (014605) (2011).
- [11] R. A. Forrest, Development of Activation Data Libraries for Fusion, http://kinr.kiev.ua/NPAE_Kyiv2008/.../Forrest_6-6.pdf.
- [12] C.H.M. Broeders, A.Yu. Konobeyev, Yu A. Korovin, et al., ALICE/ASH manual, FZK 7183, May 2006. <http://bibliothek.fzk.de/zb/berichte/FZKA7183.pdf>.
- [13] V.F. Weisskopf, D.H. Ewing, *Phys. Rev.* 57 (1940) 472.
- [14] M. Blann, H.K. Vonach, *Phys. Rev. C* 28 (1983) 1475–1492.
- [15] M. Korkmaz, M. Yiğit, O. Agar, *Acta Physica Polonica A* 132 (2017) 670–673.
- [16] M. Yiğit, *Appl. Radi. Isot.* 130 (2017) 109–114.
- [17] A.V. Ignatyuk, G.M. Smirenkin, A. Tishin, *Sov. J. Nucl. Phys.* 21 (1975) 255.
- [18] A.V. Ignatyuk, K.K. Istekov, G. Smirenkin, *Yadernaja Fizika* 29 (1979) 875.
- [19] S.K. Kataria, V.S. Ramamurthy, M. Blann, T.T. Komoto, *Nucl. Instrum. Methods Phys. Res. Sect. A* 288 (1990) 585–588.
- [20] Experimental Nuclear Reaction Data, EXFOR Data Files, 2015. <http://www.nndc.bnl.gov/exfor/exfor.htm>.
- [21] A.J. Koning, D. Rochman, S. van der Marck, et al., TENDL Database: TALYS-based Evaluated Nuclear Data Library, https://tendl.web.psi.ch/tendl_2015/tendl2015.html.
- [22] B. Canbula, *Nucl. Instrum. Methods in Phys. Res. B* 391 (2017) 73.
- [23] S. Kailas, S.K. Gupta, M.K. Mehta, et al., *Phys. Rev. C* 12 (1975) 1789.
- [24] C.H. Johnson, C.C. Trail, A. Galonsky, *Phys. Rev.* 136 (1964) B1719.
- [25] R.D. Albert, *Phys. Rev.* 115 (1959) 925.
- [26] L.F. Hansen, R.D. Albert, *Phys. Rev.* 128 (1962) 291.
- [27] G. Chodil, R.C. Jopson, H. Mark, et al., *Nucl. Phys. A* 93 (1967) 648.
- [28] R.A. Sharp, R.M. Diamond, G. Wilkinson, *Phys. Rev.* 101 (1956) 1493.
- [29] F. Ditroi, F. Tarkanyi, S. Takacs, et al., *J. Radioanal. Nucl. Chem.* 298 (2013) 853.
- [30] P.C. Johnson, M.C. Lagunas-Solar, M.J. Avila, *Appl. Radiat. Isot.* 35 (1984) 371.
- [31] R. Michel, M. Gloris, H.J. Lange, et al., *Nucl. Phys. A* 322 (1979) 40.
- [32] F.J. Haasbroek, J. Steyn, R.D. Neirinckx, et al., *Council f.Scient. Indust. Res. Pretoria* 28 (1976) 533. Repts. No.89.